Applied Physics Letters

RESEARCH ARTICLE | FEBRUARY 16 2024

Terahertz and far infrared radiation generation in air plasma created by bichromatic subpicosecond laser pulses

D. Buožius ; G. Balčas ; V. Tamulienė ; I. Babushkin ; U. Morgner ; V. Vaičaitis

Check for updates

Appl. Phys. Lett. 124, 071113 (2024)
https://doi.org/10.1063/5.0188581

View Online
Export Citation

05 July 2024 08:19:44

AIP Publishing

Applied Physics Letters ARTICLE pubs.aip.org/aip/apl

Terahertz and far infrared radiation generation in air plasma created by bichromatic subpicosecond laser pulses

Cite as: Appl. Phys. Lett. **124**, 071113 (2024); doi: 10.1063/5.0188581
Submitted: 11 December 2023 · Accepted: 30 January 2024 ·
Published Online: 16 February 2024

View Online Export Citation CrossMark

D. Buožius,[1] G. Balčas,[1] V. Tamulienė,[1,a)] I. Babushkin,[2,3,4] U. Morgner,[2,3,4] and V. Vaičaitis[1]

AFFILIATIONS

[1]Laser Research Center, Vilnius University, Saulėtekio 10, Vilnius LT-10223, Lithuania
[2]Institute of Quantum Optics, Leibniz University Hannover, Welfengarten 1, 30167 Hannover, Germany
[3]Max Born Institute, Max-Born-Strasse 2a, 10117 Berlin, Germany
[4]Cluster of Excellence PhoenixD, Welfengarten 1, 30167 Hannover, Germany

[a)]Author to whom correspondence should be addressed: viktorija.tamuliene@ff.vu.lt

ABSTRACT

Here, we report on terahertz (THz) radiation generation in air driven by the fundamental and second harmonic of Yb:KGW laser pulses with durations of a few hundred femtoseconds. It was found that the spectrum of generated THz pulses surprisingly spans up to 50 THz, which is comparable to that usually obtained using much shorter Ti:sapphire laser pulses. The broad bandwidth is attributed to a strong spatiotemporal reshaping of the pump pulses in a filament. The achieved energy conversion efficiency is comparable to the one usually obtained from much shorter pump pulses and could be further improved by an optimized experimental setup. The obtained results indicate that compact Yb-based sources provide an attractive alternative to much larger and expensive laser systems.

© 2024 Author(s). All article content, except where otherwise noted, is licensed under a Creative Commons Attribution (CC BY) license (http://creativecommons.org/licenses/by/4.0/). https://doi.org/10.1063/5.0188581

05 July 2024 08:19:44

Currently, terahertz-related technologies are widely used in various fields of science and industry, such as spectroscopy, security, biomedicine, and material analysis.[1–5] However, the search for efficient and cost-effective methods of pulsed terahertz radiation generation still remains a challenging task.[6,7] Among the laser-based methods of terahertz generation, a THz emission from laser-created gas plasmas[8] seems to be the most promising one. It can provide THz pulses with up to 150 MV cm^{-1} field strength and spectral width of 75 THz.[9,10] However, most of such THz generation systems are based on femtosecond Ti:sapphire lasers,[7] which are bulky and expensive. In contrast, commercially available Yb-based lasers are much smaller and less expensive, but they can only provide pulses of longer duration (approximately a few hundred femtoseconds). This fact makes Yb:KGW lasers less attractive for THz radiation generation in gas plasmas, since the pump pulse duration is one of the main parameters determining the efficiency of generation and spectral width of the THz pulses.[11] Note that recently an ytterbium-based laser amplifier had been used for generation of THz pulses with bandwidth up to 60 THz and peak electric field as high as 55 kV/cm.[12] However, before the plasma creation, the laser pulses of 170 fs duration first were spectrally broadened in an Ar-filled hollow-core capillary fiber and then recompressed down to about 18 fs, which again makes the laser system quite bulky and expensive. In contrast, in this paper, we demonstrate that the subpicosecond pulses from an Yb:KGW laser can be directly used for the efficient generation of broadband THz radiation in air. Our comprehensive numerical simulations, supporting the experimental results, indicate that unusually broad and efficient THz radiation is rooted in the spatiotemporal reshaping of the pump pulses caused by nonlinear propagation.

For the experiments, we used the fundamental and second harmonic (FH, SH) pulses of an Yb:KGW laser ("Pharos," Light conversion Ltd.) with an output power of up to 6 W, a central wavelength around 1030 nm and an output beam diameter of about 2 mm (at $1/e^2$ level). A laser pulse repetition rate could be tuned between 1 and 200 kHz, the pulse duration was about 190 fs (at FWHM), and the maximal available single pulse energy at the fundamental frequency for pulse repetition rates below 6 kHz was 1 mJ. The polarization of laser radiation (both the FH and SH) was kept linear in all cases during the experiment.

The experimental setup is shown in Fig. 1. First, a nonlinear beta-barium borate (BBO) crystal was inserted into the fundamental beam

© Author(s) 2024

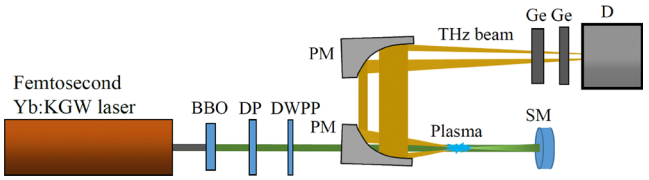

FIG. 1. Experimental setup. BBO: second harmonic generating crystal; DP: group velocity delay compensation plate; DWPP: dual wavelength phase plate; PM: parabolic metal coated off-axis mirror; SM: aluminum coated spherical mirror; Ge: germanium wafer; and D: pyroelectric detector.

path for type-I frequency doubling.[13] As a result, the pump beam consisted of the FH and SH waves with orthogonal polarizations. Since it is well known that maximal THz radiation generation is achieved with parallel polarizations, a dual wavelength phase plate (DWPP) is inserted into the pump beam path, rotating the SH polarization by 90 degrees. A temporal walk-off of the FH and SH pulses was compensated by a birefringent group velocity delay compensation plate (delay plate, DP, which delays FH pulses with respect to SH ones[14]). The pump pulses were passed through a hole in a parabolic mirror (PM) and focused by the metallic spherical mirror (SM). As a result, a faint plasma spot was created, where THz radiation generation took place. In order to minimize optical aberrations, the pump beam was reflected almost backward by the spherical mirror. The parabolic mirror PM collected and collimated the THz radiation. Note that despite its hole, this mirror was capable to collect most of THz radiation, which usually has a form of a hollow cone with a few degrees of apex angle.[15,16] The second parabolic mirror was used to focus the collimated THz beam onto a pyroelectric detector D (TPR-A-65 THz, Spectrum Detector Inc.), sensitive in the range of $0.1 - 300$ THz. THz radiation was separated from the residual pump with a few 1 mm-thick Ge wafers.

The power of generated THz radiation was measured for several experimental conditions: we have used two pump focusing mirrors (SM) of different focal lengths (10 and 15 cm) and three nonlinear BBO crystals of different thicknesses (0.5, 1.5, and 2 mm). The results are summarized in Table I, which shows that the maximum THz generation efficiency was registered using a 0.5 mm-thick crystal and mirror of 15 cm focal length.

As it was expected,[17,18] the efficiency of generation strongly depended on the pump power and the relative phase between the FH and SH pulses, which could be varied by moving the BBO crystal along the pump beam (Fig. 2).

Note that in Fig. 2 the distance between two adjacent maxima is about 60 mm, which is much larger than that registered previously (about 26 mm) using the shorter pump wavelengths of femtosecond Ti:sapphire lasers.[17,18] This can be easily explained by the fact that the

TABLE I. THz power dependence on the focal length of pump focusing mirror and thickness of the BBO crystal (laser power and pulse repetition rate were 6 W and 6 kHz, respectively).

	Crystal thickness		
Focal length	0.5 mm	1.5 mm	2 mm
10 cm	12.8 μW	11 μW	8.5 μW
15 cm	21.4 μW	11.3 μW	9.4 μW

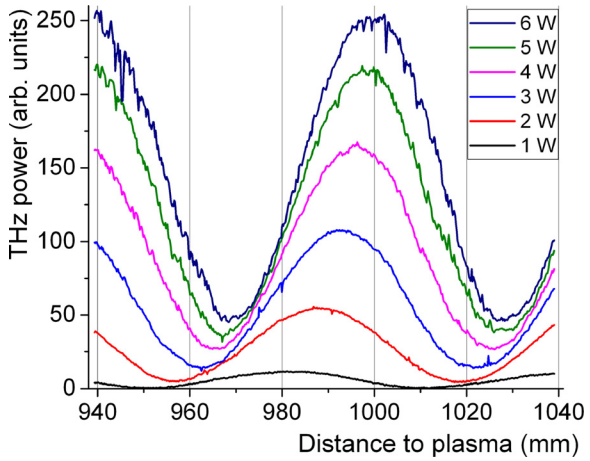

FIG. 2. Dependence of THz yield on the distance between the BBO crystal and the plasma for different pump powers (pulse repetition rate and focal length of focusing mirror were 6 kHz and 15 cm, respectively).

air dispersion for the Ti:sapphire laser wavelengths (approximately 800 and 400 nm) is much larger than that for the Yb:KGW laser wavelengths (1030 and 515 nm). More specifically, according to the transient photocurrent model,[10] THz yield is maximal when the phase difference between the FH and SH waves is $\theta = \pm\pi/2$. Since during propagation in air, the phase difference varies in the following way $\theta = \omega(n_\omega - n_{2\omega})d/c + \theta_0$,[10,19] where d is the distance of propagation, n_ω and $n_{2\omega}$ are the refractive indices of air at frequencies ω and 2ω, respectively, c is the speed of light in vacuum, and θ_0 is the phase difference just after the BBO crystal, the distance between two maxima Δd can be easily calculated as being proportional to the pump wavelength divided by the difference of refractive indices of FH and SH. For the wavelengths of 1030/515 nm, this difference is nearly by a factor of 1.7 smaller than that for the wavelengths of 800/400 nm (4.52×10^{-6} and 7.71×10^{-6}, respectively[20]). Taking into account the wavelength ratio (about 1.29), one can arrive to the conclusion that the distance between neighboring maxima should be larger by a factor of about 2.2, which is the case in our experiment. Note that the optimal position of the nonlinear crystal was clearly dependent on the pump power, which is caused by the plasma-induced nonlinear phase shifts of the FH and SH pulses.[17,21]

We have also measured the THz yield as a function of the repetition rate (Fig. 3) at constant laser pulse energies. Here, the THz power grows almost linearly with the pump pulse repetition rate up to 40 kHz, when saturation starts. At low repetition rates, the time interval between two adjacent pump pulses is large and these pulses do not interact with each other; therefore, the linear scaling of THz yield is to be expected. However, we believe that at repetition rates above 40 kHz, the thermal interaction of adjacent pulses starts, i.e., the first pulses are heating the air volume, where the consecutive pulses generate plasma and THz radiation. This results in some defocusing of the pump beam and phase shifts between the FH and SH waves.[22] Therefore, above 40 kHz, the THz yield no longer follows linear law, but still grows as the thermal losses are partially compensated by the bigger number of pump pulses. Note that in order to avoid these thermal effects, all other measurements were performed at 6 kHz repetition rate.

05 July 2024 08:19:44

© Author(s) 2024

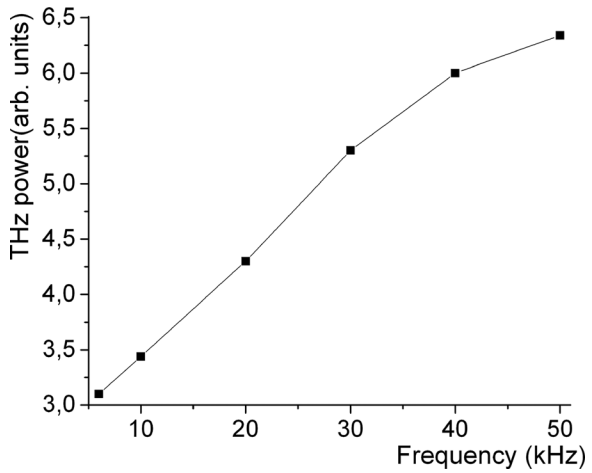

FIG. 3. Dependence of THz power as a function of the laser repetition rate. Single pulse energy and focal length of the focusing mirror were 0.12 mJ and 15 cm, respectively.

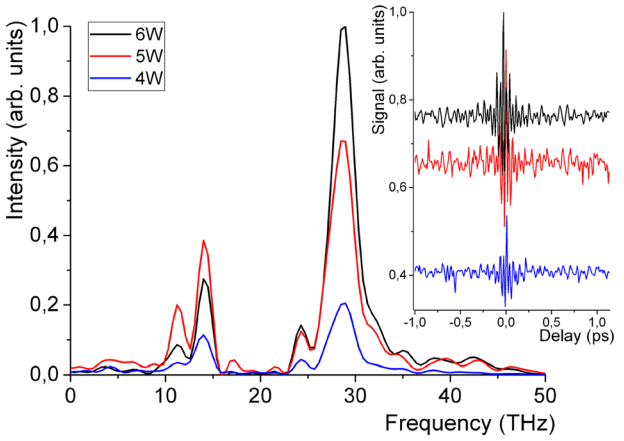

FIG. 4. Measured spectra of THz radiation for laser powers of 4, 5, and 6 W. Inset shows the corresponding interference traces.

The spatial distribution of the THz radiation was measured under optimum conditions (BBO thickness 0.5 mm, SM focal length 15 cm, and average power 6 W). Then, the THz detector D behind a small aperture was moved across the collimated beam, and the position dependent THz power was collected. With the focal length of the parabolic mirror (PM, Fig. 1), these data were recalculated to the THz beam angular distribution, which was included into the numerically obtained graphs shown below.

Note that the observed apex angle of the THz cone (about 6°) is larger than that known from the Ti:sapphire laser experiments.[15,16] In short, this is explained by the dispersion properties of air: the pump pulses of longer wavelengths propagate faster and as a Cherenkov-type emission, the apex angle of generated THz cone becomes larger.[23–25] Indeed, the cone angle θ of Cherenkov-type emission is defined by $\cos\theta = u_{\mathrm{THz}}/V$, where u_{THz} is the group velocity at THz frequency and V is the velocity of the pump X wave.[25] Thus, the angle θ increases with V.

THz spectra were registered using a home-made THz Michelson interferometer along with the THz detector D.[26] By moving one arm of the interferometer, we have registered interferometric traces of the THz pulses, and then through a fast Fourier transform obtained the corresponding intensity spectra presented in Fig. 4. Note that significant spectral intensity spans from a few THz to more than 50 THz. Thus, the spectral width of the THz pulses generated in air by the long Yb:KGW laser pulses is comparable to that usually obtained with much shorter Ti:sapphire laser pulses (up to 75 THz[10,16,27]). Furthermore, the low frequency part of the spectrum is underestimated due to the transmission of the Ge wafers[28] as well as elimination of the spectral components at smaller angles than 3°, see the description of Fig. 6.

We estimated that the maximum THz energy conversion efficiency was more than 10^{-6}, which again is comparable to that usually obtained by using much shorter pulses of femtosecond Ti:sapphire lasers. However, such conversion efficiency is by at least one order of magnitude lower than that obtained using much shorter (about 18 fs) pump pulses at the same wavelength.[12] The further improvement is possible by optimizing the pump focusing and BBO thickness. Note that we cannot directly compare THz generation efficiency of our sub-picosecond laser with the conventional femtosecond systems at different wavelengths of laser radiation since the efficiency depends on the pump wavelength.[29–31] In addition, it was recently shown that circularly polarized FH and SH pulses could produce by a factor of 3–5 more powerful THz pulses than that in the linear case.[32,33] Therefore, one may expect further increase in the conversion efficiency at least by an order of magnitude. In addition, as our simulations show (see below), the low-frequency part (below 15 THz) can be also significant, so that using more suitable filter can increase the detected THz yield by another order of magnitude.

Here, we simulate the governing equation that involves the linear propagation term as well as the nonlinear $\chi^{(3)}$, plasma current, and nonlinear absorption terms. The governing equation is written for the Fourier transform $\widehat{\mathcal{E}}(\omega, \beta_r, z)$ of the analytic signal $\mathcal{E}(t, r, z)$, and the electric field is given by $E = \mathrm{Re}(\mathcal{E})$, where $\mathrm{Re}(^\circ)$ denotes the real part, while t, r, and z are the time, radial, and longitudinal coordinates in the cylindrical coordinate system. Then,

$$\frac{\partial\widehat{\mathcal{E}}}{\partial z} = iK_z\widehat{\mathcal{E}} + i\widehat{P}_{\mathrm{Kerr}} - i\widehat{P}_{\mathrm{pl}} - \widehat{P}_{\mathrm{loss}}. \quad (1)$$

The linear propagation term $iK_z\widehat{\mathcal{E}}$ is estimated by the use of the formula $K_z = [k^2(\omega) - \beta_r^2]^{1/2} - \omega/u_{10}$, where $k(\omega) = \frac{\omega n(\lambda)}{c}$, $n(\lambda)$ is the wavelength dependent refractive index found from the Sellmeier equation of air,[20] c is the speed of light, and $i = \sqrt{-1}$. u_{10} is the group velocity of the fundamental wave. The linear propagation term describes both the pulse dispersion and beam diffraction. The nonlinear $\chi^{(3)}$ term is given by $\widehat{P}_{\mathrm{Kerr}} = \frac{4}{3}n_2\varepsilon_0\omega\mathrm{FT}[\mathrm{Re}(\mathcal{E})^3]$, where $\mathrm{FT}[\bigcirc]$ denotes the Fourier transform operation, $n_2 = 4\times10^{-23}$ m^2/W is the nonlinear refractive index of air, and ε_0 is the vacuum permittivity. The plasma term is given by $\widehat{P}_{\mathrm{pl}} = \frac{e^2}{2m_e c\varepsilon_0}\frac{1}{\omega+i\nu_c}\mathrm{FT}[\rho\mathcal{E}]$, where e and m_e are the electron charge and mass, respectively. $\nu_c = 1/200$ fs^{-1} is the collision frequency, and ρ is the plasma density. The nonlinear losses are accounted by

05 July 2024 08:19:44

© Author(s) 2024

$$\widehat{P}_{\text{loss}} = \text{FT}\left([0.2W_{O_2}(t)U_{O_2} + 0.8W_{N_2}(t)U_{N_2})] \frac{\rho_0 - \rho}{\text{Re}(\mathcal{E})2\varepsilon_0 c} \right), \quad (2)$$

where the ionization energies of the main constituents of air oxygen and nitrogen are U_{O_2} and U_{N_2}, respectively. W_{O_2,N_2} is the corresponding emission rate calculated using the Yudin–Ivanov formula,[34] and ρ_0 is the number density of air.

The nonlinear propagation terms were assumed to be nonzero at $\omega > 0$. Plasma current and nonlinear absorption terms contain the plasma density that is described by the additional equation,

$$\frac{\partial \rho}{\partial t} = (\rho_0 - \rho)(0.2W_{O_2}(t) + 0.8W_{N_2}(t)). \quad (3)$$

The Yudin–Ivanov formula for the ionization rate includes both multiphoton and tunnel ionization processes. Although it holds only for the single-colored wave, the whole analytic signal $\mathcal{E}$ including the weak second harmonic was used in the calculations. Note that only the tunnel, but not the multiphoton ionization produces the THz radiation,[35] because to produce harmonics (including THz), one needs the free electron densities changed on the sub-cycle scale. This is automatically taken into account in our model. Also, increasing the ponderomotive energy with the wavelength is also automatically taken into account in our model for the ionization current as it was shown in Ref. 36.

The boundary condition of Eq. (1) is given by

$$\mathcal{E}(t, r, z = 0) = A_{10}(t, r)\exp(i\omega_0 t) + A_{20}(t, r)\exp(2i\omega_0 t), \quad (4)$$

where input complex amplitudes of fundamental and second harmonics are given by

$$A_{j,0}(t, r) = a_{j,0}\exp\left(-2\ln(2)\frac{t^2}{\tau_0^2} - \frac{r^2}{r_0^2}\right)\exp\left(i\frac{\pi r^2}{\lambda_{0,jf}}\right). \quad (5)$$

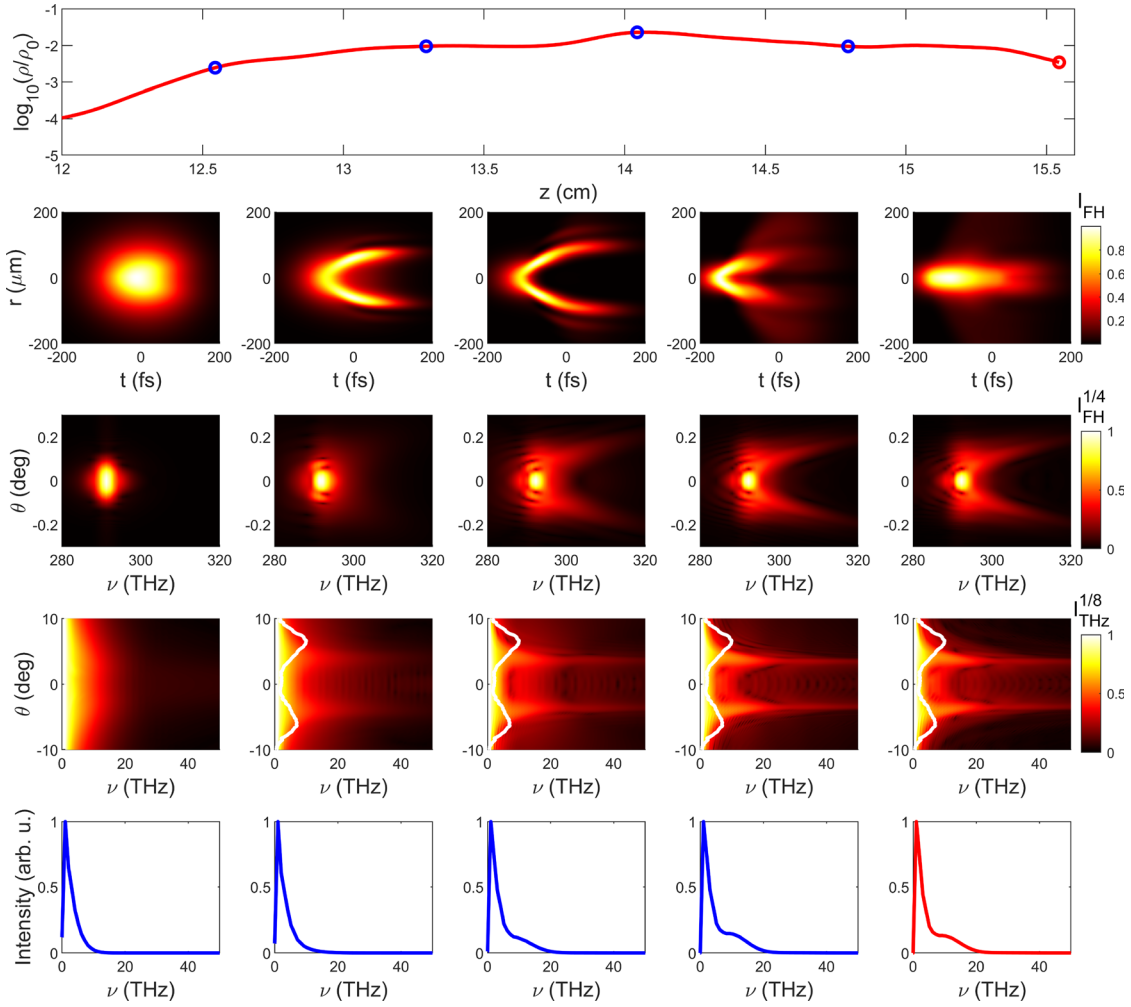

FIG. 5. Numerically simulated evolution of the plasma density in the vicinity of the lens focus (first row), fundamental intensity distribution (second row) and spectrum (third row), spectrum of the THz radiation (fourth row), and integrated frequency spectrum of THz radiation (fifth row). White line in fourth row: experimental angular distribution of THz radiation. Propagation distances, corresponding to every particular column of the subfigures, are indicated by the circles in the upper subfigure.

05 July 2024 08:19:44

© Author(s) 2024

Here, the indexes $j = 1$ and $j = 2$ stand for the fundamental and second harmonics, respectively, τ_0 and r_0 are the pulse duration [at the full width half maximum (FWHM)] and beam radius (at $1/e^2$ level), respectively. Both beams are focused by a lens of focal length f. $\lambda_{0,j}$ is the central wavelength, and $a_{j,0}$ is the input amplitude.

Numerical simulation of Eq. (1) with boundary condition of Eq. (4) has been performed utilizing the split-step Fourier transform method[37] with Runge–Kutta fourth method for the nonlinear step. Since the cylindrical symmetry was assumed, the Hankel transform[38] in the space domain was performed. In the time domain, Fourier transform was applied. We set the following parameters: $\lambda_{01} = 1030$ nm, $f = 15$ cm, $\tau_0 = 190$ fs, and $2r_0 = 2$ mm, intensity fraction $a_{2,0}^2/a_{1,0}^2 = 0.1$, and input energy $E_0 = 1.2$ mJ. The time domain $t \in [-3\tau_0\ 3\tau_0)$ was divided in 8192 equal steps, and space domain $r \in (0\ 2r_0]$ was divided in 400 steps. The longitudinal step h_z was varied with propagation. At the beginning, $h_z = f/100$ and the vicinity of focus, at $z > 0.75 \times f$, $h_z = f/20\,000$. The results are presented in Fig. 5.

It illustrates an evolution of plasma density with propagation in the vicinity of the lens focus (the first row) as well as the FH intensity distribution (the second row) and FH angular-frequency spectra (the third row) along with the angular-frequency spectra of THz radiation (the fourth row) and integrated over spatial frequency THz spectra (the fifth row) for various propagation distance values, marked by the blue circles in the first row. The most interesting result is the strong spectral broadening of THz radiation (fourth and fifth rows) with the evolution of the FH pulse shape (second row). In the plasma filament, the fundamental pulse duration estimated at specific coordinate is smaller than the initial one, second row. The FH spectrum obeys a broad-spectrum part, third row. As a result, conical broadband THz radiation is generated, fourth and fifth rows. The conical structure of the THz radiation is seen in the fourth row. Here, we also put the experimental curve of the angular intensity distribution at THz frequencies (shown as a white line) in order to compare the theoretical and experimentally obtained angular structures of THz emission. The conical structure of generated THz radiation is in a tight connection with FH and SH X-waves (superluminal localized pulses that obey certain dispersion relation and are X-shaped[39]) propagation in air plasma.[25] The broadband part of FH spectrum evidences the presence of X-wave. On the other hand, the broadening of the pump spectra causes the broadening of the THz spectrum, too.

The calculated conversion efficiency at the output was 7×10^{-4}. The large difference between experimental and theoretical conversion efficiencies is caused by the low transmission of Ge filters and the fact that during the experiment the power of THz beam was registered only for angles larger than 3°. In Fig. 6, we are presenting transmission spectrum of used Ge wafers and show that the observed spectrum must be significantly modified by two used Ge windows as well as by the neglection of the small-angle contribution. This effect suppresses the lowest frequencies, so that higher frequency range becomes mode visible, so, as a result, two-lobe structure appears. However, in the experiment (cf. Fig. 4), the second lobe seems much more pronounced and shifted to somewhat higher frequencies. We attribute this to the fact that lower frequencies have much higher divergence and some of the lowest frequencies escape the detector.

In conclusion, we have demonstrated the efficient generation of broadband THz radiation from air excited by subpicosecond pulses of

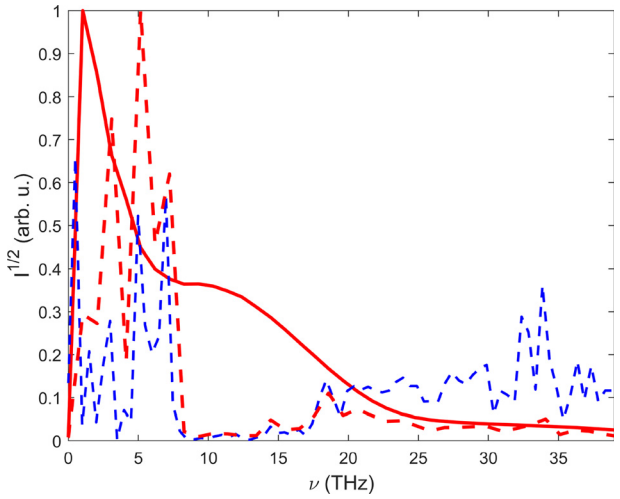

FIG. 6. Numerically simulated output THz spectrum (red solid line), transmission of Ge wafer (blue dashed line), and the first spectrum multiplied by the square of the second spectrum and smaller angles than 3° excluded (red dashed line).

Yb:KGW laser. THz radiation obtained from such sources possess, in contrast to expectations, a rather broad spectrum up to 50 THz, and high efficiency, both comparable to the THz emission, produced by much shorter pump pulses. This is a result of the strong spatiotemporal reshaping of the pump pulse as it passes through the focus. Since the Yb:KGW lasers are significantly smaller and less expensive than the usually used femtosecond Ti:sapphire lasers, our report demonstrates the potential for development of compact low-cost THz sources and systems based on THz emission from laser-created air plasmas and two-color filamentation in liquids, where recently[40] it was demonstrated a remarkably high conversion efficiency exceeding 10^{-3}.

This project has received funding from the European Union's Horizon 2020 research and innovation programme under Grant Agreement No. 871124 Laserlab-Europe. This study was performed under the "Universities' Excellence Initiative" programme. I.B. and U.M. are thankful for funding by the Deutsche Forschungsgemeinschaft (DFG, German Research Foundation) under Germany's Excellence Strategy within the Cluster of Excellence PhoenixD (EXC 2122, Project ID 390833453).

AUTHOR DECLARATIONS

Conflict of Interest

The authors have no conflicts to disclose.

Author Contributions

D. Buožius: Investigation (equal). **G. Balčas:** Investigation (equal). **Viktorija Tamulienė:** Investigation (equal); Writing – original draft (equal). **I. Babushkin:** Investigation (equal); Writing – review & editing (equal). **U. Morgner:** Writing – review & editing (equal). **V. Vaičaitis:** Methodology (equal); Resources (equal); Writing – original draft (equal).

05 July 2024 08:19:44

© Author(s) 2024

DATA AVAILABILITY

The data that support the findings of this study are available from the corresponding author upon reasonable request.

REFERENCES

[1]M. Tonouchi, "Cutting-edge terahertz technology," Nat. Photonics **1**, 97–105 (2007).
[2]P. Siegel, "Terahertz technology," IEEE Trans. Microwave Theory Tech. **50**, 910–928 (2002).
[3]M. Hangyo, "Development and future prospects of terahertz technology," Jpn. J. Appl. Phys., Part 1 **54**, 120101 (2015).
[4]M. Naftaly, N. Vieweg, and A. Deninger, "Industrial applications of terahertz sensing: State of play," Sensors **19**, 4203 (2019).
[5]P. Bawuah and J. A. Zeitler, "Advances in terahertz time-domain spectroscopy of pharmaceutical solids: A review," TrAC Trends Anal. Chem. **139**, 116272 (2021).
[6]R. A. Lewis, "A review of terahertz sources," J. Phys. D **47**, 374001 (2014).
[7]Y. Zhang, K. Li, and H. Zhao, "Intense terahertz radiation: Generation and application," Front. Optoelectron. **14**, 4–36 (2021).
[8]D. J. Cook and R. M. Hochstrasser, "Intense terahertz pulses by four-wave rectification in air," Opt. Lett. **25**, 1210–1212 (2000).
[9]A. D. Koulouklidis, C. Gollner, V. Shumakova, V. Yu. Fedorov, A. Pugžlys, A. Baltuška, and S. Tzortzakis, "Observation of extremely efficient terahertz generation from mid-infrared two-color laser filaments," Nat. Commun. **11**, 292 (2020).
[10]K. Y. Kim, A. J. Taylor, J. H. Glownia, and G. Rodriguez, "Coherent control of terahertz supercontinuum generation in ultrafast laser–gas interactions," Nat. Photonics **2**, 605–609 (2008).
[11]H. Roskos, M. Thomson, M. Kreß, and T. Löffler, "Broadband THz emission from gas plasmas induced by femtosecond optical pulses: From fundamentals to applications," Laser Photonics Rev. **1**, 349–368 (2007).
[12]R. Piccoli, A. Rovere, Y.-G. Jeong, Y. Jia, L. Zanotto, F. Légaré, B. E. Schmidt, R. Morandotti, and L. Razzari, "Extremely broadband terahertz generation via pulse compression of an ytterbium laser amplifier," Opt. Express **27**, 32659–32665 (2019).
[13]R. W. Boyd, *Nonlinear Optics* (Elsevier Science, 2003).
[14]See https://www.newlightphotonics.com/Time-Delay-Compensators-Ultrafast for "Time Delay Compansators at Newlight Photonics Inc."
[15]H. Zhong, N. Karpowicz, and X.-C. Zhang, "Terahertz emission profile from laser-induced air plasma," Appl. Phys. Lett. **88**, 261103 (2006).
[16]V. Vaičaitis, M. Ivanov, K. Adomavičius, Ž. Svirskas, U. Morgner, and I. Babushkin, "Influence of laser-preformed plasma on THz wave generation in air by bichromatic laser pulses," Laser Phys. **28**, 095402 (2018).
[17]V. Pyragaitė, V. Smilgevičius, K. Steponkevičius, B. Makauskas, and V. Vaičaitis, "Phase shifts in terahertz wave generation by tightly focused bichromatic laser pulses," J. Opt. Soc. Am. B **31**, 1430–1435 (2014).
[18]D. Dietze, J. Darmo, S. Roither, A. Pugzlys, J. N. Heyman, and K. Unterrainer, "Polarization of terahertz radiation from laser generated plasma filaments," J. Opt. Soc. Am. B **26**, 2016–2027 (2009).
[19]T. I. Oh, Y. S. You, N. Jhajj, E. W. Rosenthal, H. M. Milchberg, and K. Y. Kim, "Intense terahertz generation in two-color laser filamentation: Energy scaling with terawatt laser systems," New J. Phys. **15**, 075002 (2013).
[20]P. E. Ciddor, "Refractive index of air: New equations for the visible and near infrared," Appl. Opt. **35**, 1566–1573 (1996).
[21]V. Tamulienė, D. Buožius, and V. Vaičaitis, "Plasma-assisted temporal shifts of bichromatic femtosecond laser pulses in air," Phys. Rev. A **103**, 033502 (2021).
[22]N. Jhajj, Y. Cheng, J. K. Wahlstrand, and H. M. Milchberg, "Optical beam dynamics in a gas repetitively heated by femtosecond filaments," Opt. Express **21**, 28980–28986 (2013).
[23]V. Vaičaitis, "Cherenkov-type phase-matched third harmonic generation in air," Opt. Commun. **185**, 197–202 (2000).
[24]L. A. Johnson, J. P. Palastro, T. M. Antonsen, and K. Y. Kim, "THz generation by optical cherenkov emission from ionizing two-color laser pulses," Phys. Rev. A **88**, 063804 (2013).
[25]D. Buožius, B. Motiejūnas, V. Vaičaitis, and V. Tamulienė, "Emission of conical THz radiation induced by bichromatic pump *X* waves in an air plasma," Phys. Rev. A **105**, 023521 (2022).
[26]V. Vaičaitis, O. Balachninaitė, A. Matijošius, I. Babushkin, and U. Morgner, "Direct time-resolved plasma characterization with broadband terahertz light pulses," Phys. Rev. E **107**, 015201 (2023).
[27]M. Ivanov, I. Thiele, L. Bergé, S. Skupin, D. Buožius, and V. Vaičaitis, "Intensity modulated terahertz vortex wave generation in air plasma by two-color femtosecond laser pulses," Opt. Lett. **44**, 3889–3892 (2019).
[28]V. Rogalin, I. Kaplunov, and G. Kropotov, "Optical materials for the THz range," Opt. Spectrosc. **125**, 1053–1064 (2018).
[29]A. Nguyen, K. J. Kaltenecker, J. Delagnes, B. Zhou, E. Cormier, N. Fedorov, R. Bouillaud, D. Descamps, I. Thiele, S. Skupin, P. U. Jepsen, and L. Bergé, "Wavelength scaling of terahertz pulse energies delivered by two-color air plasmas," Opt. Lett. **44**, 1488–1491 (2019).
[30]M. Clerici, M. Peccianti, B. E. Schmidt, L. Caspani, M. Shalaby, M. Giguère, A. Lotti, A. Couairon, F. Légaré, T. Ozaki, D. Faccio, and R. Morandotti, "Wavelength scaling of terahertz generation by gas ionization," Phys. Rev. Lett. **110**, 253901 (2013).
[31]A. Nguyen, P. González de Alaiza Martínez, J. Déchard, I. Thiele, I. Babushkin, S. Skupin, and L. Bergé, "Spectral dynamics of THz pulses generated by two-color laser filaments in air: The role of Kerr nonlinearities and pump wavelength," Opt. Express **25**, 4720–4740 (2017).
[32]Y.-Y. Tu, C. Meng, X. Sun, H.-Z. Wu, P. Song, C.-S. Meng, X.-W. Wang, Z.-Y. Zhou, Z.-H. Lyu, D.-W. Zhang, Z.-X. Zhao, and J.-M. Yuan, "Enhancement of terahertz radiation from a filament by using circularly polarized two-color laser fields," J. Opt. Soc. Am. B **39**, A83–A88 (2022).
[33]C. Tailliez, A. Stathopulos, S. Skupin, D. Buožius, I. Babushkin, V. Vaičaitis, and L. Bergé, "Terahertz pulse generation by two-color laser fields with circular polarization," New J. Phys. **22**, 103038 (2020).
[34]G. L. Yudin and M. Y. Ivanov, "Nonadiabatic tunnel ionization: Looking inside a laser cycle," Phys. Rev. A **64**, 013409 (2001).
[35]I. Babushkin, C. Brée, C. M. Dietrich, A. Demircan, U. Morgner, and A. Husakou, "Terahertz and higher-order Brunel harmonics: From tunnel to multiphoton ionization regime in tailored fields," J. Mod. Opt. **64**, 1078–1087 (2017).
[36]I. Babushkin, S. Skupin, and J. Herrmann, "Generation of terahertz radiation from ionizing two-color laser pulses in Ar filled metallic hollow waveguides," Opt. Express **18**, 9658–9663 (2010).
[37]M. S. Wartak, *Computational Photonics. An Introduction With MATLAB* (Cambridge University Press, 2013), pp. 357–360.
[38]P. Banerjee, G. Nehmetallah, and M. Chatterjee, "Numerical modeling of cylindrically symmetric nonlinear self-focusing using an adaptive fast Hankel split-step method," Opt. Commun. **249**, 293–300 (2005).
[39]E. Recami, M. Zamboni-Rached, and H. E. Hernández Figueroa, "Localized waves: A historical and scientific introduction," in *Localized Waves* (Wiley, Hoboken, NJ, 2008).
[40]I. Dey, K. Jana, V. Yu. Fedorov, A. D. Koulouklidis, A. Mondal, M. Shaikh, D. Sarkar, A. D. Lad, S. Tzortzakis, A. Couairon, and G. R. Kumar, "Highly efficient broadband terahertz generation from ultrashort laser filamentation in liquids," Nat. Commun. **8**, 1184 (2017).

05 July 2024 08:19:44

© Author(s) 2024